Thermal conductivity in *B*- and *C*- phases of UPt_3

P. Thalmeier[1] and K. Maki[2,3]
[1]*Max Planck Institute for the Chemical Physics of Solids, Nöthnitzer Strasse 40, 01187 Dresden, Germany*
[2]*Max Planck Institute for the Physics of Complex Systems, Nöthnitzer Strasse 38, 01187 Dresden, Germany*
[3]*Department of Physics and Astronomy, University of Southern California, Los Angeles, California 90089-0484*
(Received 10 July 2002; published 31 March 2003)

Although the superconductivity in UPt_3 is one of the most well studied, there are still lingering questions about the nodal directions in the *B* and *C* phases in the presence of a magnetic field. Limiting ourselves to the low-temperature regime $[T \ll \Delta(0)]$, we study the magnetothermal conductivity within semiclassical approximation using Volovik's approach. The angular dependence of the magnetothermal conductivity for an arbitrary field direction is calculated for both phases. We show that cusps in the polar angle dependence appear in *B* and *C* phases that are due to the polar point nodes.

DOI: 10.1103/PhysRevB.67.092510 PACS number(s): 74.20.Rp, 74.25.Fy, 74.70.Tx

Perhaps due to the exceptional appearance of two superconducting (sc) transitions with two associated critical field curves, UPt_3 is one of the most well studied heavy fermion superconductors. The history of this subject was described in Ref. 1. The *T* linear dependence of the low-temperature thermal conductivity both parallel to the *c* axis and the *a* axis was in favor of the E_{2u}- rather than E_{1g}-type sc order parameter,[2–4] a discussion of the latter is therefore no longer necessary in the present work. Further Pt NMR experiments confirmed the triplet nature of the superconductivity and the details of the triplet gap function $\mathbf{d}(\mathbf{k})$ in *A*, *B*, and *C* phases were determined.[5,6] This assignment of the spin configuration is consistent with the weak spin-orbit coupling limit[6–8] also assumed here. H_{c2} along the c axis requires a strong Pauli limiting effect.[9] This favors strong spin-orbit coupling but then H_{c2} results are inconsistent with the NMR data. We assume that $\mathbf{d}(\mathbf{k}) = \Delta(\mathbf{k})\hat{z}$ to be weakly pinned along *c*. Then the E_{2u} gap functions of for the low-temperature *B* and *C* phases of UPt_3 are given by

$$\Delta(\vartheta,\varphi) = \tfrac{3}{2}\sqrt{3}\Delta \cos\vartheta \sin^2\vartheta \exp(\pm 2i\varphi), \quad B \text{ phase}$$
$$\Delta(\vartheta,\varphi) = \tfrac{3}{2}\sqrt{3}\Delta \cos\vartheta \sin^2\vartheta \cos(2\varphi), \quad C \text{ phase}. \tag{1}$$

Here ϑ and φ are the polar and azimuthal angles of $\mathbf{k}$. The angular dependence of $\Delta(\vartheta,\varphi)$ is shown in Fig. 1. In the *B* phase the poles are second-order node points and the equator is a node line. In the *C* phase two additional vertical nodal lines appear at 45° away from the vertical plane containing $\mathbf{H}$. The thermal conductivity dependence on field strength for field along the symmetry axis also decided in favor of the E_{2u} state against the E_{1g} state;[10] this is reviewed in Ref. 11. A much more powerful method for studing the nodal structure of the gap is the investigation of the field-*angle* dependence of thermal conductivity in the vortex phase, because the location and type of extrema allow a direct determination of the node type and positions with respect to crystal axes. This method is the main topic of the present work and we make detailed predictions for UPt_3. Existing experimental results on angular dependent thermal conductivity[12] have been analyzed in Ref. 13. Unfortunately the experiment was done for $T > 0.3$ K, which is not sufficiently low to determine node structures. Recently we have been studying the angle-dependent thermal conductivity in other nodal superconductors.[14–19] Here we shall restrict ourselves to the low-temperature limit $T \ll \tilde{v}\sqrt{eH} \ll \Delta(0)$ and the superclean limit $(\Gamma\Delta)^{1/2} \ll \tilde{v}\sqrt{eH}$, where $\tilde{v} = (v_a v_c)^{1/2}$, Γ is the scattering rate in the unitarity limit, and $v_{a,c}$ are the anisotropic Fermi velocities. The condition $\tilde{v}\sqrt{eH} \ll \Delta(0)$ can be satisfied in the *B* phase while $\tilde{v}\sqrt{eH} \leqslant \Delta(0)$ in the *C* phase, since the latter appears only for $H \geqslant 0.6$ T and $H \geqslant 1.2$ T for field along *a* and *c*, respectively. Our results in the *C* phase may therefore only have qualitative significance. Restriction to the superclean limit does not influence the main conclusions on the connection between node topology and magnetothermal conductivity. We first examine the quasiparticle density of states (DOS) and the thermodynamic properties of the *B* and *C* phase of UPt_3 in the presence of a magnetic field with arbitrary orientation at low temperatures. Then we study the thermal conductivity in the *B* and *C* phase in the low-temperature regime, which provides clear evidence for the nodal positions in $\Delta(\mathbf{k})$. In this regime the influence of the antiferromagnetic order in UPt_3 may be neglected contrary to the *A*-phase regime.

The quasiparticle DOS in the vortex state of UPt_3 is given by

$$g(0) = \mathrm{Re}\left\langle \frac{C_0 - ix}{\sqrt{(C_0 - ix)^2 + f^2}} \right\rangle, \tag{2}$$

where the angular brackets denote both Fermi surface and vortex lattice averages. With the form factor $f_B(z) = (3\sqrt{3}/2)(1-z^2)z$ and $f_C(z,z') = (2z'^2 - 1)f_B(z)$ $(z = \cos\vartheta,\ z' = \cos\varphi)$ for *B* and *C* phases, respectively, the average may be computed, and one obtains

$$g_B(0) = \frac{1}{\sqrt{3}}\left\{ \frac{\pi}{2}x + C_0\left\langle \left[\ln\left(\frac{C_0}{x}\right) - 1 \right] \right\rangle \right\},$$

$$g_C(0) = \frac{1}{\sqrt{3}}\left[\frac{\pi}{2}\left\langle x \ln\left(\frac{2}{x}\right) \right\rangle + \frac{2}{\pi}C_0\left\langle \ln^2\left(\frac{2}{x}\right) \right\rangle \right], \tag{3}$$

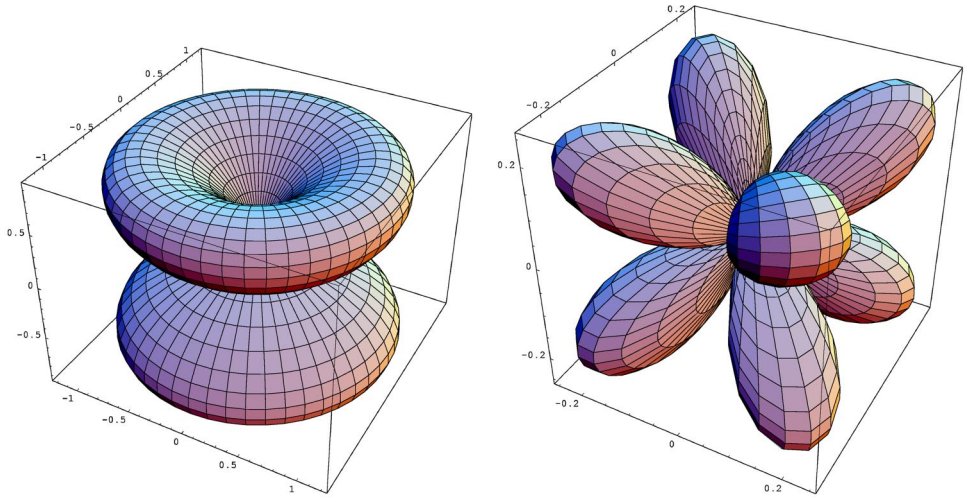

FIG. 1. Spherical plots of $|\Delta(\vartheta,\varphi)|$ for the B phase (left) and C phase (right). For the C phase two additional vertical nodal planes appear an angle $\pi/4$ away from the vertical plane, which contains **H** assumed at $\phi=\pi/4$.

where $x=|\mathbf{v}\cdot\mathbf{q}|/\Delta$ is the normalized Doppler shift of quasiparticle energies, $C_0=\lim_{\omega\to 0}\mathrm{Im}(\tilde{\omega}/\Delta)$ and $\tilde{\omega}$ is the renormalized quasiparticle energy in the presence of impurity scattering.[14,20] Furthermore, **v** is the quasiparticle velocity and $2\mathbf{q}$ is the pair momentum around the vortex. The second terms in Eq. (3) are neglected due to the superclean condition $x\gg C_0$, then Γ does not appear in the field dependence. Following Volovik[21] we obtain

$$\langle x\rangle_B=\frac{2}{\pi}\tilde{v}\frac{\sqrt{eH}}{\Delta}I_B(\theta),$$

$$\left\langle x\ln\left(\frac{2}{x}\right)\right\rangle_C=\frac{2}{\pi}\tilde{v}\frac{\sqrt{eH}}{\Delta}I_C(\theta)\ln\left(\frac{\Delta}{\tilde{v}\sqrt{eH}}\right), \tag{4}$$

$$I_B(\theta)=\alpha\sin\theta+\frac{2}{\pi}E(\sin\theta),\quad I_C(\theta)=I_B(\theta)+I(\theta).$$

Here $E(\sin\theta)$ is the complete elliptic integral of the second kind. Furthermore, we used the definition

$$I(\theta)=\frac{1}{2}\left\{\frac{f(\theta)}{\sqrt{|1-\alpha^2\sin^2\theta|}}+2\alpha\sin\theta+\cos\theta\left(\frac{\pi}{2}-\tan^{-1}(\alpha\tan\theta)\right)\right\},$$

$$f(\theta)=\begin{cases}\cos^{-1}(\alpha\sin\theta) & \text{for } \sqrt{\alpha}\,\sin(\theta)<1\\ \cosh^{-1}(\alpha\sin\theta) & \text{for } \sqrt{\alpha}\,\sin(\theta)>1,\end{cases} \tag{5}$$

where $\alpha=v_c/v_a$ is the anisotropy of Fermi velocities and θ is the polar angle of **H** with respect to c axis. The averages in Eq. (4) are evaluated by replacing the **k** space integration by a summation over nodal positions and then integrating out the superfluid velocity field.[13,14] We assume a square vortex lattice for simplicity; a hexagonal lattice would lead to an additional numerical factor 0.93.

Substituting Eq. (4) into Eq. (3), we obtain

$$g_B=\frac{1}{\sqrt{3}}\tilde{v}\frac{\sqrt{eH}}{\Delta}I_B(\theta),$$

$$g_C=\frac{2}{\pi\sqrt{3}}\tilde{v}\frac{\sqrt{eH}}{\Delta}I_C(\theta)\ln\left(\frac{\Delta}{\tilde{v}\sqrt{eH}}\right). \tag{6}$$

In addition, we have $C_0=(\Gamma/\Delta)[g(0)]^{-1}$. The low-temperature specific heat, the spin susceptibility, etc., are given by

$$\frac{C_s}{\gamma_N T}=\frac{\chi_s}{\chi_N}=1-\frac{\rho_s(H)}{\rho_s(0)}=g(0), \tag{7}$$

where ρ_s is the superfluid density. The θ dependence of $g(0)$ for B and C phases is shown in Figs. 2 and 3, respectively.

The thermal conductivity tensor in the vortex phase depends on the angles (θ,ϕ) of **H** due to the angle dependence of the Doppler shift energy Δx. Here ϕ is the azimuthal angle between **H** and the direction of the heat current $\mathbf{j}_Q$ in the ab plane. Following Ref. 19 we obtain for the B phase

$$\frac{\kappa_{zz}}{\kappa_n}=\frac{2}{3}\frac{v_a v_c}{\Delta^2}(eH)I_B(\theta)F_B^{zz}(\theta),$$

$$\frac{\kappa_{xx}}{\kappa_n}=\frac{1}{3}\frac{v_a^2}{\Delta^2}(eH)I_B(\theta)F_B^{xx}(\theta),$$

$$F_B^{zz}(\theta)=\sin\theta,$$

$$F_B^{xx}(\theta,\phi)=\frac{2}{\pi}\left[\sin^2\phi\,E(\sin\theta)+\cos(2\phi)\frac{1}{3\sin^2\theta}\times[\cos^2\theta\,K(\sin\theta)-\cos(2\theta)E(\sin\theta)]\right]. \tag{8}$$

For fields along symmetry directions the linear field dependence of κ_{zz} has also been obtained in Ref. 22.

The thermal Hall coefficient in the B phase is obtained as

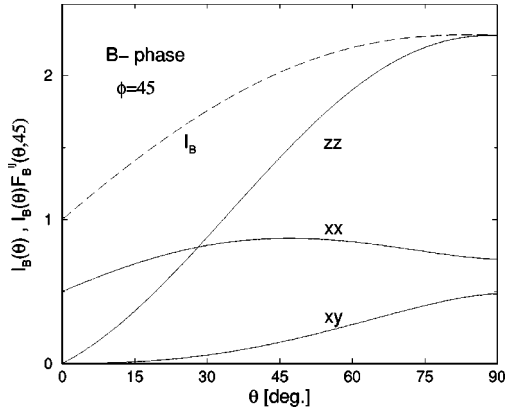

FIG. 2. Polar field-angle dependence of $I_B(\theta)$ and $I_B(\theta)F_B^{ij}(\theta,45°)$ $(ij=xx,zz,xy)$ that determines the θ dependence of DOS $g(0)$, thermal conductivities $(\kappa_{xx},\kappa_{zz})$ and thermal Hall coefficient (κ_{xy}).

$$\frac{\kappa_{xy}}{\kappa_n}(\theta)=-\frac{v_a^2(eH)}{3\Delta^2}I_B(\theta)F_B^{xy}(\theta,\phi),$$

$$F_B^{xy}(\theta,\phi)=\frac{2}{\pi}\frac{\sin(2\phi)}{3\sin^2\theta}[(2-\sin^2\theta)E(\sin\theta) \tag{9}$$

$$-2\cos^2\theta K(\sin\theta)].$$

The θ and ϕ angle dependences of κ_{ij} $(ij=xx,zz,xy)$ in the B phase are shown in Fig. 2 and Fig. 4. For heat current along c (κ_{zz}) no ϕ dependence appears. In the limit $\theta=\pi/2$, $I_B(\pi/2)=\alpha+2/\pi$ and then

$$\kappa_{xx}\sim\frac{1}{\pi}\left(1-\frac{1}{3}\cos(2\phi)\right);\quad \kappa_{xy}\sim\frac{2}{3\pi}\sin(2\phi). \tag{10}$$

The maximum in $\kappa_{xx}(90°,\phi)$ at $\phi=\pm 90°$ occurs for heat current $\perp\mathbf{H}$ when the Doppler shift gives rise to the largest quasiparticle DOS parallel to the heat current and we have $\kappa_{xx}(\phi=90°)/\kappa_{xx}(\phi=0°)=2$.

Now we consider the C phase. Again κ_{zz} does not exhibit a ϕ dependence. The C phase according to Eq. (1) has two additional perpendicular node lines. Rotating the field at a

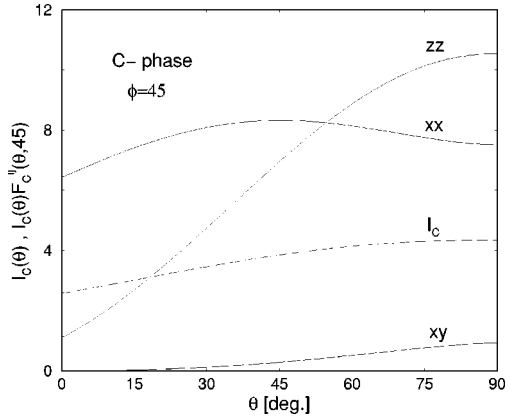

FIG. 3. Polar field-angle dependence of $I_C(\theta)$ and $I_C(\theta)F_C^{ij}(\theta,45°)$ $(ij=xx,zz,xy)$.

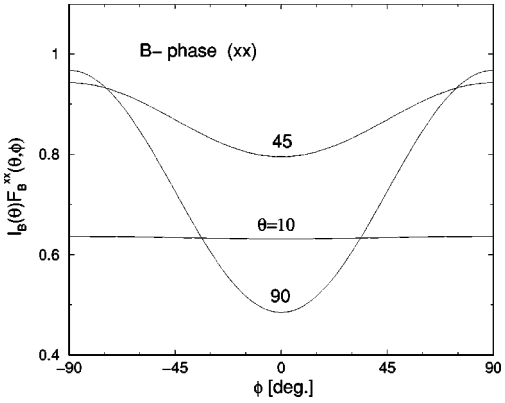

FIG. 4. Azimuthal field-angle dependence of $I_B(\theta)F_B^{xx}(\theta,\phi)$ for various θ. For $\theta\to 0°$ the ϕ dependence is suppressed completely. The zz component is always ϕ independent.

given θ around c (i.e., changing ϕ) will lead to a corotation of these node lines such that the vertical plane containing $\mathbf{H}$ always stays at a half angle between the two perpendicular planes of the node lines parallel to c (Ref. 9; see inset of Fig. 5). Consequently $\kappa_{zz}(\theta)$ will again be independent of ϕ while $\kappa_{xx}(\theta,\phi)$ depends on both field angles. We find for heat current along c:

$$\frac{\kappa_{zz}}{\kappa_n}=\frac{1}{6}\frac{v_a^2}{\Delta^2}(eH)I_C(\theta)F_C^{zz}(\theta)\ln^2\left(\frac{\Delta}{\tilde{v}\sqrt{eH}}\right), \tag{11}$$

$$F_C^{zz}(\theta)=\alpha\sin\theta+\frac{2}{\pi}\int_{-1}^{1}dz|z|\left[\frac{1}{2}(1+\cos^2\theta)(1-z^2)\right.$$

$$\left.+(\alpha^2\sin^2\theta z^2+\sqrt{2}\sin\theta\cos\theta z(1-z^2)1/2\right]^{1/2}.$$

On the other hand, we obtain for the heat current along a:

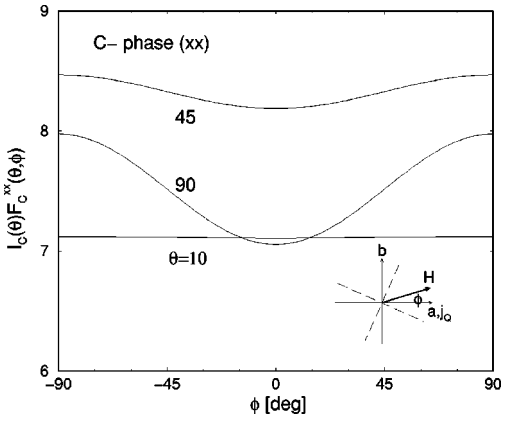

FIG. 5. Azimuthal field-angle dependence of $I_C(\theta)F_C^{xx}(\theta,\phi)$ for various θ. The zz component is again ϕ independent. The inset shows the field and node geometry in the C phase. The node lines along c are lying in the planes perpendicular to ab (dashed lines), which are mutually orthogonal. The field $\mathbf{H}$ lies at the half angle $(\pi/4)$ between forming an angle ϕ with the heat current $\mathbf{j}_Q$ along the a axis. This geometry is preserved for any ϕ because the nodal planes corotate with the field.

$$\frac{\kappa_{xx}}{\kappa_n}=\frac{1}{3\pi}\frac{v_a^2}{\Delta^2}(eH)I_C(\theta)F_C^{xx}(\theta,\phi)\ln^2\left(\frac{\Delta}{\tilde{v}\sqrt{eH}}\right),$$
$$F_C^{xx}(\theta,\phi)=F_B^{xx}(\theta,\phi)+\sqrt{2}(1+\cos^2\theta)^{1/2}. \quad (12)$$

As is readily seen κ_{zz} depends only on θ, while κ_{xx} depends both on θ and ϕ. Both angular dependences are shown in Fig. 3 and Fig. 5, respectively.

In both B and C phases κ_{ij} $(ij=xx,zz)$ and also the specific heat, which is determined by $I_{B,C}$, exhibit clear cusps at the poles $\theta=0$ (and $\theta=\pi$) caused by the contributions from the respective second-order node points that are present in both B and C phases. This is very similar to what has been recently observed and analyzed in YNi_2B_2C.[23] There the second-order node points lie along the equator and hence the cusps appear as function of ϕ. The most significant difference in the B- and C-phase results can be seen in the behavior of κ_{zz} for small polar angle θ. While in the B phase it approaches zero, it remains finite in the C phase. Furthermore the $\kappa_{xx}-\kappa_{zz}$ anisotropy for $\theta=\pi/2$ is considerably smaller in the C phase as compared to the B phase. In both B and C phases the xx component exhibts nonmonotonic behavior as function of θ.

The thermal Hall coefficient in the C phase reads

$$\frac{\kappa_{xy}}{\kappa_n}(\theta)=-\frac{v_a^2}{3\Delta^2}(eH)I_C(\theta)F_C^{xy}(\theta,\phi)\ln^2\left(\frac{\Delta}{\tilde{v}\sqrt{eH}}\right), \quad (13)$$

where $F_C^{xy}(\theta,\phi)=F_B^{xy}(\theta,\phi)$ holds because the contributions from perpendicular node lines with **H** lying at the half angle between cancel and so as in the B phase one is left with polar and equatorial contributions to the thermal Hall constant. For numerical calculations we used the anisotropy ratio $\alpha=v_c/v_a=1.643$. It can be directly obtained from experimental anisotropies of thermal and electrical conductivities[1] $\sigma_c/\sigma_a=\sigma_c/\sigma_a=2.7$, which are equal to α^2.

We have found that in UPt_3 at low temperatures (i.e., $T\ll\tilde{v}\sqrt{eH}$) and in the superclean limit $[(\Gamma\Delta)^{1/2}\ll\tilde{v}\sqrt{eH}]$, the thermal conductivity exhibits a clear angular dependence that will help to identify the nodal directions in $\Delta(\mathbf{k})$ and to verify the predictions of the commonly discussed E_{2u} model for the gap function in B and C phases. Most significantly we predict that (i) cusps appear in the thermal conductivity and specific heat for $\theta=0°$ (and $\theta=\pi$) due to the polar point nodes of UPt_3 in both B and C phases, (ii) in the C phase for heat current along the nodal direction ($\phi=\pi/4$) a finite $\kappa_{zz}(\theta,\pi/4)$ occurs even for $\theta\to0$, which is caused by the contribution from the additional perpendicular node regions (for the B phase this contribution vanishes), (iii) the $\kappa_{xx}-\kappa_{zz}$ anistropy for **H** in the ab plane ($\theta=\pi/2$) is considerably larger in the B phase as compared to the C phase. This is again caused by the perpendicular node lines that contribute and enhance κ_{xx} only for the C phase.

We hope that these different features in the field-angle-dependent thermal conductivity tensor above and below the critical field of the B-C transition will resolve a part of the remaining controversy surrounding $\Delta(\mathbf{k})$ in UPt_3. We recall that thermal conductivity experiments have been very useful to identify $\Delta(\mathbf{k})$ in unconventional superconductors. For example Izawa *et al.* have succeded to identify $\Delta(\mathbf{k})$ in Sr_2RuO_4,[24] $CeCoIn_5$,[25] organic salts,[26] and more recently YNi_2B_2C.[23] Indeed the thermal conductivity appears to provide a unique window to access the nodal structure in unconventional superconductors.

We would like to thank Koichi Izawa and Yuji Matsuda for useful discussions.

[1] R. Joynt and L. Taillefer, Rev. Mod. Phys. **74**, 235 (2002).
[2] B. Lussier *et al.*, Phys. Rev. B **53**, 5145 (1996).
[3] M. R. Norman and P. J. Hirschfeld, Phys. Rev. B **53**, 5706 (1996).
[4] M. J. Graf *et al.*, J. Low Temp. Phys. **102**, 367 (1996); **106**, 727(E) (1996).
[5] H. Tou *et al.*, Phys. Rev. Lett. **77**, 1374 (1996).
[6] H. Tou *et al.*, Phys. Rev. Lett. **80**, 3129 (1998).
[7] Y. Kitaoka *et al.*, Physica B **281&282**, 878 (2000).
[8] K. Machida *et al.*, J. Phys. Soc. Jpn. **10**, 3361 (1999).
[9] G. Yang and K. Maki, Europhys. Lett. **48**, 208 (1999).
[10] M. Houssa and M. Ausloos, Phys. Rev. Lett. **79**, 2879 (1997).
[11] J. P. Brison *et al.*, Physica B **281-282**, 872 (2000).
[12] H. Suderow *et al.*, Phys. Lett. A **234**, 64 (1997).
[13] K. Maki *et al.*, Physica C **341-348**, 1647 (2000).
[14] H. Won and K. Maki, cond-mat/0004105 (unpublished).
[15] T. Dahm *et al.*, cond-mat/0006301 (unpublished).
[16] H. Won and K. Maki, Appl. Current Phys. **1**, 291 (2001).
[17] H. Won and K. Maki, Europhys. Lett. **52**, 427 (2000); **54**, 248 (2001).
[18] P. Thalmeier and K. Maki, Europhys. Lett. **58**, 119 (2002).
[19] K. Maki *et al.*, Phys. Rev. B **65**, 140502(R) (2002).
[20] G. Yang and K. Maki, Eur. Phys. J. B **21**, 61 (2001).
[21] G. E. Volovik, Pis'ma Zh. Éksp. Teor. Fiz. **58**, 457 (1993) [JETP Lett. **58**, 469 (1993)].
[22] Yu. S. Barash and A. A. Svidzinsky, Phys. Rev. B **58**, 6476 (1998).
[23] K. Izawa *et al.*, Phys. Rev. Lett. **89**, 137006 (2002).
[24] K. Izawa *et al.*, Phys. Rev. Lett. **86**, 2653 (2001).
[25] K. Izawa *et al.*, Phys. Rev. Lett. **87**, 057002 (2001).
[26] K. Izawa *et al.*, Phys. Rev. Lett. **88**, 027002 (2002).